The Astronomical Journal, 129:1818–1826, 2005 April

OPTICAL MONITORING OF BL LACERTAE OBJECT S5 0716+714 WITH HIGH TEMPORAL RESOLUTION

Jianghua Wu, Bo Peng, Xu Zhou, Jun Ma, Zhaoji Jiang, and Jiansheng Chen
National Astronomical Observatories, Chinese Academy of Sciences, 20A Datun Road,
Beijing 100012, China; jhwu@bao.ac.cn, pb@bao.ac.cn, zhouxu@bac.pku.edu.cn
Received 2004 November 19; accepted 2005 January 5

ABSTRACT

Optical monitoring of S5 0716+714 was performed with a 60/90 Schmidt telescope in 2003 November and December and 2004 January for studying the variability of the object on short timescales. Because of the high brightness of the source, we could carry out quasi-simultaneous measurements in three bands with a temporal resolution of about 20 minutes by using one single telescope. Intraday and intranight variations were observed, showing an overall change of $\sim$0.9 mag during the whole campaign. Two outbursts were recorded on Julian Dates 2,453,005 and 2,453,009. Minimum timescales of a few hours were derived from the light curves of individual nights, but they were different from night to night. A bluer-when-brighter chromatism was present when the object was showing a fast flare but was absent when it was in a relatively quiescent state. Our results are basically consistent with the shock-in-jet model and demonstrate that geometric effects can sometimes play an important role in the variability of blazars.

Key words: BL Lacertae objects: individual (S5 0716+714) — galaxies: active — galaxies: jets — galaxies: photometry

Online material: machine-readable tables

1. INTRODUCTION

Blazars are a subset of active galactic nuclei (AGNs). These radio-loud flat-spectrum objects exhibit the most rapid and largest amplitude variations among all AGNs. The variations are thought to originate from a relativistic jet, which is believed to be at a small angle to our light of sight and which is probably powered and accelerated by a rotating and accreting supermassive black hole. There are basically two types of blazars, BL Lac objects and flat-spectrum radio quasars; the former have a featureless optical continuum, while the latter show many strong, broad emission lines.

Variability studies of blazars have been essential in understanding the physics of their central regions, which in general cannot be resolved even with existing or planned optical/infrared interferometers. The timescales, spectral changes, and correlations and delays between variations in different continuum components provide crucial information on the nature and location of these components and on their interdependencies. These parameters can be well studied with multifrequency observational campaigns, such as those coordinated for Mrk 421 (e.g., Buckley et al. 1996), 3C 279 (e.g., Wehrle et al. 1998), S5 0716+714 (e.g., Raiteri et al. 2003; Wagner et al. 1996), and PKS 2155−304 (e.g., Urry et al. 1997).

The BL Lac object S5 0716+714 is well known for its intraday variability (IDV) in the radio and optical bands and has been the target of many monitoring programs, as mentioned above. Nesci et al. (2002) found a typical variation rate of 0.02 mag hr^{-1} and a maximum rising rate of 0.16 mag hr^{-1} for this object. Heidt & Wagner (1996) reported a period of 4 days in the optical band, while Qian et al. (2002) derived a 10 day period from their 5.3 yr optical monitoring. The latter authors also discovered a variation range of about 3 mag in the V band and 2.5 mag in both the R and I bands during their whole monitoring program. The optical and radio behavior of the object was recently presented by Raiteri et al. (2003), based on 8 years of optical and more than 20 years of radio observations. Four major optical outbursts were observed at the beginning of 1995, in late 1997, at the end of 2000, and in fall 2001. An exceptional brightening of 2.3 mag in 9 days was detected in the R band just before a *BeppoSAX* pointing on 2000 October 30. The radio flux variations at different frequencies are similar, but the amplitude decreases with increasing wavelength. Its multiwavelength variability was described in detail in Wagner et al. (1996).

The broadband spectral properties of S5 0716+714 seem to be between those of a low-frequency-peaked and a high-frequency-peaked BL Lac object (Ulrich et al. 1997). The high-energy part of its spectral energy distribution is expected to peak in the MeV energy domain. A 450 ks *INTEGRAL* observation of S5 0716+714 proposed by the Landessternwarte Heidelberg group (principal investigator: S. Wagner) was performed from 2003 November 10 to 18. A number of ground-based radio and optical telescopes monitored this source during this period, including our 60/90 Schmidt telescope.

Our monitoring program covered the period from 2003 November 8 to 18 and from 2003 December 30 to 2004 January 5 with a temporal resolution of about 20 minutes. Unlike most previous investigations, which focused on the long-term variability of this object, we concentrated on its microvariability on short timescales because of our high temporal resolution. The short timescales and spectral behaviors were studied. Here we present the observational results and analysis.

This paper is organized as follows: The observation and reduction procedures for the monitoring data are described in § 2. Section 3 presented the results, including the light curves, the analysis of the timescales and spectral changes, and some discussion on the sinelike light curves we observed. A summary is given in § 4.

2. OBSERVATION AND DATA REDUCTION

Our optical monitoring program was performed on a 60/90 Schmidt telescope located at the Xinglong Station of the

TABLE 1

OBSERVATIONAL LOG AND RESULTS IN THE BATC *e* BAND IN PERIOD 1

Observation Date (UT)[a]	Observation Time (UT)[a]	Exposure Time (s)	JD	*e* (mag)	e_{err} (mag)
2003 11 08	16:04:57	100	2452952.171	14.285	0.026
2003 11 08	17:43:46	300	2452952.241	14.329	0.014
2003 11 08	18:19:14	300	2452952.265	14.327	0.014
2003 11 08	18:54:11	300	2452952.289	14.312	0.013
2003 11 12	16:36:29	300	2452956.194	14.522	0.014

NOTES.—Table 1 is published in its entirety in the electronic edition of the *Astronomical Journal*. A portion is shown here for guidance regarding its form and content.

[a] The obs. date and time are of universal time. They are the same for Tables 3–7.

TABLE 2

OBSERVATIONAL LOG AND RESULTS IN THE BATC *f* BAND IN PERIOD 1

Observation Date (UT)	Observation Time (UT)	Exposure Time (s)	JD	*f* (mag)	f_{err} (mag)
2003 11 08	16:16:03	100	2452952.178	14.221	0.022
2003 11 08	17:51:25	300	2452952.246	14.247	0.012
2003 11 08	18:26:52	300	2452952.270	14.272	0.012
2003 11 08	19:01:50	300	2452952.295	14.234	0.011
2003 11 08	19:29:07	300	2452952.314	14.256	0.011

NOTES.—Table 2 is published in its entirety in the electronic edition of the *Astronomical Journal*. A portion is shown here for guidance regarding its form and content.

TABLE 3

OBSERVATIONAL LOG AND RESULTS IN THE BATC *k* BAND IN PERIOD 1

Observation Date (UT)	Observation Time (UT)	Exposure Time (s)	JD	*k* (mag)	k_{err} (mag)
2003 11 08	16:33:17	100	2452952.190	13.869	0.021
2003 11 08	18:11:18	300	2452952.260	13.882	0.010
2003 11 08	18:46:28	300	2452952.284	13.879	0.010
2003 11 08	19:21:27	300	2452952.308	13.867	0.010
2003 11 08	19:48:44	300	2452952.327	13.869	0.010

NOTES.—Table 3 is published in its entirety in the electronic edition of the *Astronomical Journal*. A portion is shown here for guidance regarding its form and content.

TABLE 4

OBSERVATIONAL LOG AND RESULTS IN THE BATC *e* BAND IN PERIOD 2

Observation Date (UT)	Observation Time (UT)	Exposure Time (s)	JD	*e* (mag)	e_{err} (mag)
2003 12 30.....	12:31:07	300	2453004.023	14.535	0.015
2003 12 30.....	12:42:56	300	2453004.032	14.505	0.014
2003 12 30.....	12:59:40	300	2453004.043	14.506	0.013
2003 12 30.....	13:16:10	300	2453004.055	14.514	0.014
2003 12 30.....	13:32:42	300	2453004.066	14.534	0.014

NOTES.—Table 4 is published in its entirety in the electronic edition of the *Astronomical Journal*. A portion is shown here for guidance regarding its form and content.

TABLE 5

OBSERVATIONAL LOG AND RESULTS IN THE BATC *f* BAND IN PERIOD 2

Observation Date (UT)	Observation Time (UT)	Exposure Time (s)	JD	*f* (mag)	f_{err} (mag)
2003 12 30.....	12:49:12	300	2453004.036	14.430	0.012
2003 12 30.....	13:05:58	300	2453004.047	14.445	0.012
2003 12 30.....	13:22:14	300	2453004.059	14.436	0.012
2003 12 30.....	13:38:47	300	2453004.070	14.448	0.011
2003 12 30.....	13:59:29	300	2453004.085	14.426	0.012

NOTES.—Table 5 is published in its entirety in the electronic edition of the *Astronomical Journal*. A portion is shown here for guidance regarding its form and content.

TABLE 6

OBSERVATIONAL LOG AND RESULTS IN THE BATC *i* BAND IN PERIOD 2

Observation Date (UT)	Observation Time (UT)	Exposure Time (s)	JD	*i* (mag)	i_{err} (mag)
2003 12 30.....	12:26:59	180	2453004.020	14.152	0.007
2003 12 30.....	12:38:17	180	2453004.028	14.163	0.007
2003 12 30.....	12:55:21	180	2453004.040	14.161	0.007
2003 12 30.....	13:12:06	180	2453004.051	14.164	0.007
2003 12 30.....	13:28:21	180	2453004.062	14.149	0.007

NOTES.—Table 6 is published in its entirety in the electronic edition of the *Astronomical Journal*. A portion is shown here for guidance regarding its form and content.

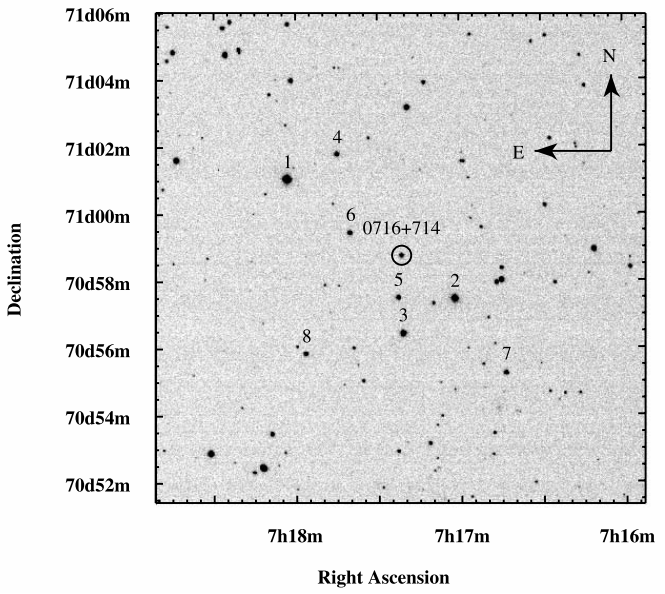

FIG. 1.—Finding chart of S5 0716+714 and the eight comparison stars taken with the 60/90 Schmidt telescope and filter *i* on JD 2,453,008. The size is $14'.5 \times 14'.5$ (or 512×512 in pixels). The eight comparison stars are the same as in Villata et al. (1998).

National Astronomical Observatories of China (NAOC). A Ford Aerospace 2048×2048 CCD camera is mounted at its main focus. The CCD has a pixel size of 15 μm, and its field of view is $58' \times 58'$, resulting in a resolution of $1''.7$ pixel^{-1}. The telescope is equipped with a 15 color intermediate-band photometric system, covering a wavelength range from 3000 to 10,000 Å. The telescope and the photometric system are mainly used to carry out the Beijing-Arizona-Taiwan-Connecticut (BATC) survey and have shown their efficiency in detecting fast variabilities in blazars (e.g., Peng et al. 2003).

The observations with the telescope are now highly automated. The telescope and filters can be controlled by a single computer command with a parameter file that specifies the telescope pointing, the filter change, the exposure time, etc. Once the observation starts, the work remaining for the observers is to check the quality of the observed CCD images and to pay attention to the weather conditions. In fact, after the night assistant prepared the hardware, the monitoring of S5 0716+714 was controlled remotely by a computer at the headquarters of NAOC in Beijing, which is about 140 km away from the telescope.

Our monitoring of S5 0716+714 was divided into two periods, one from 2003 November 8 to 18 (six nights, in fact, as a result of weather conditions) and the other from 2003 December 30 to 2004 January 5 (seven successive nights). The first period (period 1) covered the duration of the *INTEGRAL* observation, and the second period (period 2) was an extension of period 1. A filter cycle of *e*, *f*, and *k* (central wavelengths of 4873, 5248, and 7528 Å, respectively) was used in period 1, and a typical exposure time of 200–300 s was able to produce an image with a good signal-to-noise ratio. Only the central 512×512 pixels were read out for the CCD images, and the readout time was about 5.6 s. Accounting for the time for the filter changes, we achieved a temporal resolution of about 20 minutes in each band. This enabled us to realize quasi-simultaneous measurements in three BATC bands with a high temporal resolution by using only one telescope. The size of the 512×512 image is $14'.5 \times 14'.5$ and is enough to cover the BL Lac object and eight previously published comparison stars (Villata et al. 1998).

TABLE 7
BATC MAGNITUDES OF EIGHT COMPARISON STARS

Star	*e*	*f*	*i*	*k*
1	11.207	11.174	11.075	11.007
2	11.656	11.615	11.508	11.490
3	12.663	12.564	12.428	12.361
4	13.366	13.296	13.245	13.211
5	13.760	13.661	13.511	13.449
6	13.839	13.747	13.590	13.564
7	14.049	13.962	13.628	13.645
8	14.335	14.284	14.113	14.106

During period 2 we changed the *k* filter to the more sensitive *i* filter (central wavelength of 6711 Å), with which a shorter exposure time can produce images with the same quality as in the *k* band. The other observational procedures and constraints were the same as in period 1. The observational log and parameters are presented in Tables 1–6, with the observation date and time (UT), exposure time, Julian Date (JD), and BATC magnitude and error. The finding chart of S5 0716+714 and the comparison stars is illustrated in Figure 1.

In order to obtain in real time the light curves of the BL Lac object, we developed an automatic procedure. The procedure includes the following steps: The CCD images were first flat-fielded, then Bertin's SExtractor (Bertin & Arnouts 1996) was run on the CCD frames, and the instrumental magnitudes and errors of S5 0716+714 and the eight comparison stars were extracted. The average FWHM of the stellar images is about $4''.0$. A photometric aperture of 5 pixel ($8''.5$) diameter was adopted during the extraction. The BATC *e*, *f*, *i*, and *k* magnitudes of the eight comparison stars were obtained by observing them and the BATC standard star HD 19445 in the same night and are listed in Table 7. Then, by comparing the instrumental magnitudes of the eight comparison stars with their BATC magnitudes, the instrumental magnitudes of S5 0716+714 were calibrated into the BATC *e*, *f*, *i*, and *k* magnitudes, and the light curves in the four BATC bands were obtained.

3. RESULTS

3.1. *Light Curves*

The light curves are displayed in Figures 2 and 3 for periods 1 and 2, respectively. The large panels show the light curves of the BL Lac object, and the small ones present the differential magnitudes (average set to 0) between the fifth comparison star and the average of all eight. In order to show the variation clearly, we plot only the times when the BL Lac object was observed and exclude the daytime periods when no observations could be made.

All light curves show intranight fluctuations superposed on longer timescale variations. In period 1 (see Fig. 2) the variation is characterized by fast oscillations with small amplitudes. In the first night, or on JD 2,452,952, the BL Lac object was in a relatively high state. Then its brightness dropped in the following days and reached a minimum on JD 2,452,956. In the following 2 days, the BL Lac object got brighter, reaching another high state around the beginning of JD 2,452,959. The total magnitude change was about 0.4 mag in period 1, and the magnitude changes within individual nights were mostly about 0.1 mag, except for

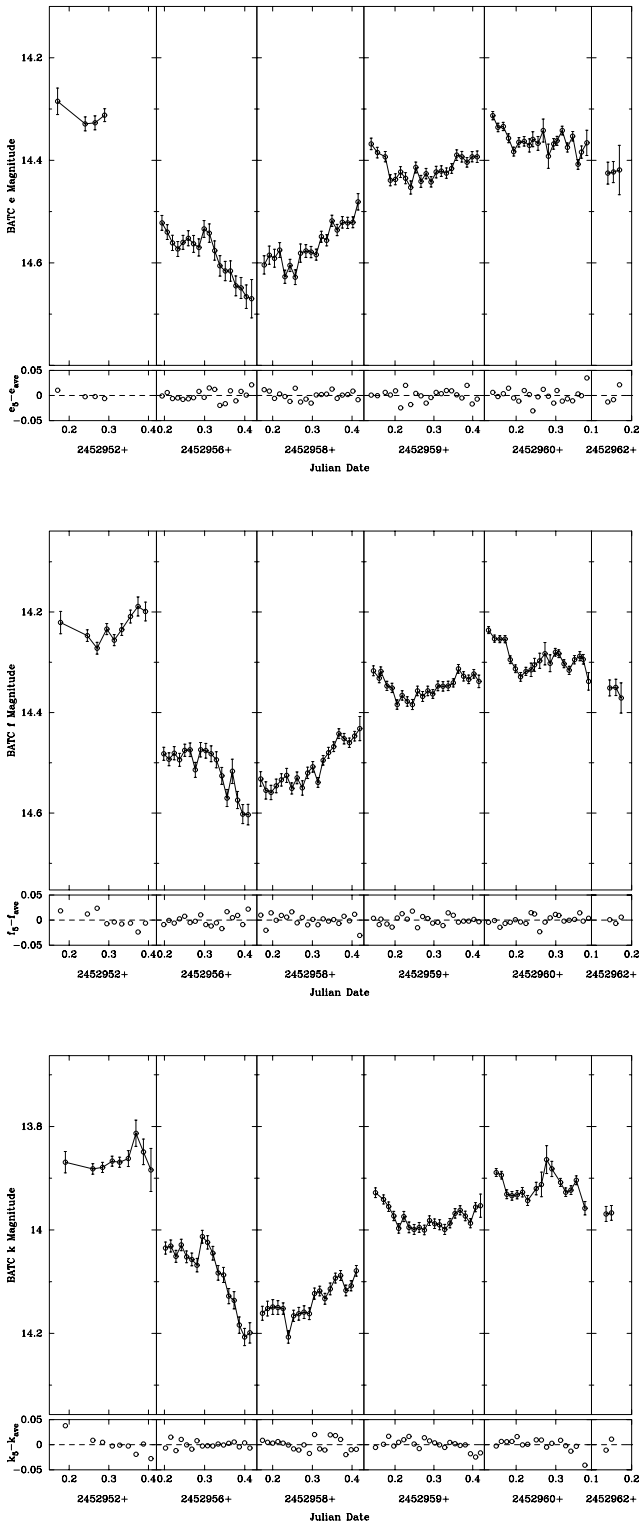

FIG. 2.—Light curves of S5 0716+714 in the BATC *e*, *f*, and *k* bands in period 1. The large panels show the light curves of the BL Lac object, and small ones show the differential magnitudes between the fifth comparison star and the average of all eight.

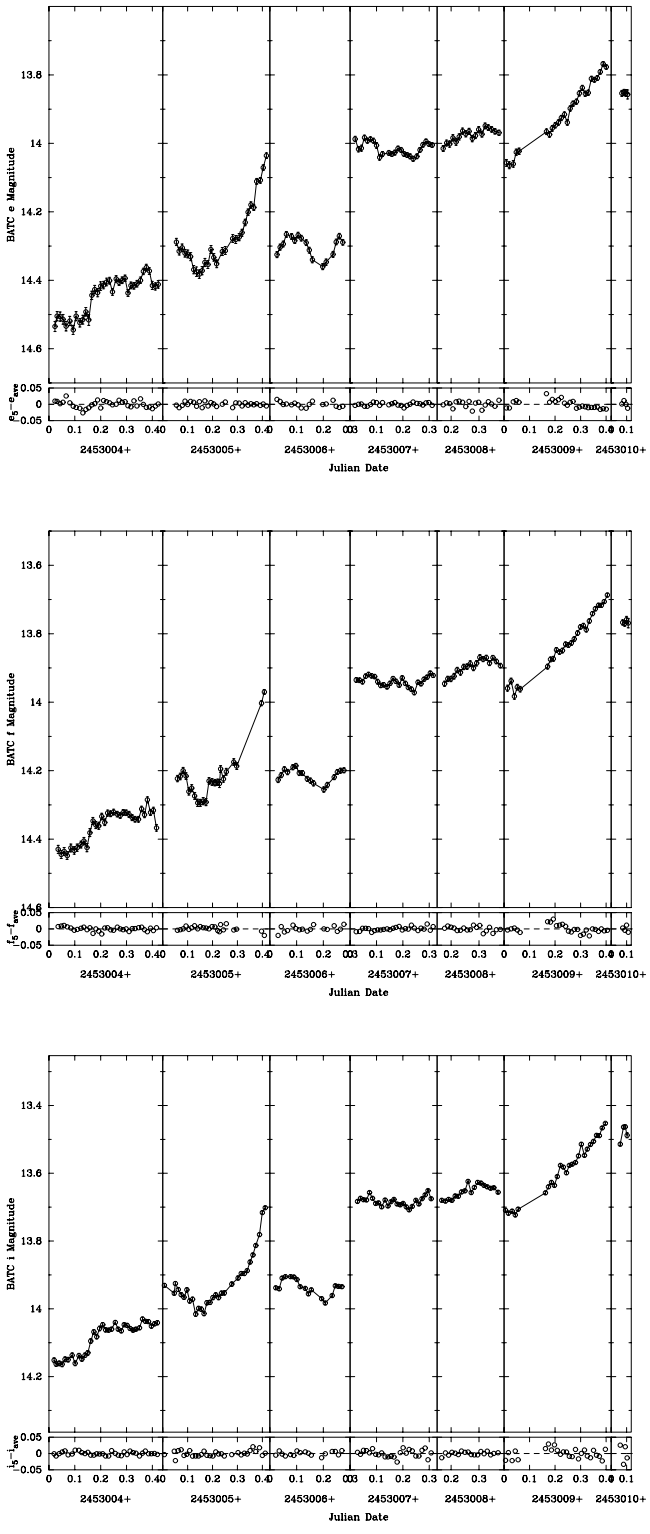

FIG. 3.—Light curves of S5 0716+714 in the BATC *e*, *f*, and *i* bands in period 2. The large panels show the light curves of the BL Lac object, and small ones show the differential magnitudes between the fifth comparison star and the average of all eight.

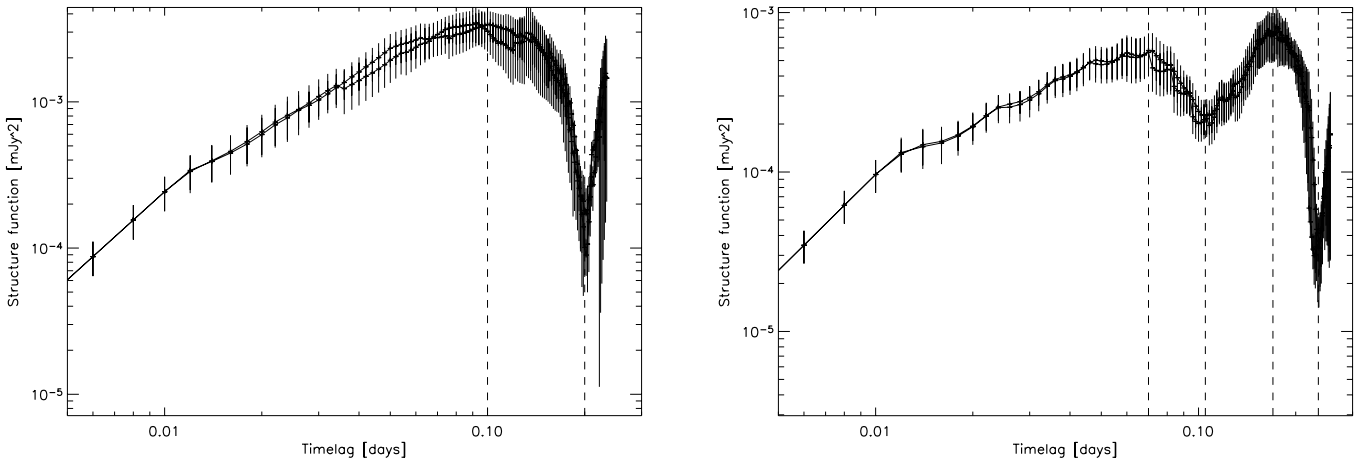

FIG. 4.—Structure function of S5 0716+714 on JD 2,453,006 (*left*) and 2,453,007 (*right*). The dashed lines indicate timescales at the maxima and periods at the minima of the structure functions.

that on JD 2,452,956. The object appeared in a relatively quiescent state.

The observational accuracy in period 2 is higher than in period 1 as a result of better weather conditions. The light curves are characterized by a continuous (except on JD 2,453,006) increase in brightness. Two outbursts were observed on JD 2,453,005 and 2,453,009 with rapid brightening of more than 0.3 mag within 0.4 days. The most sharp increase in brightness occurred on JD 2,453,005. The *i* magnitude changed from 13.896 on JD 2,453,005.328 to 13.716 on JD 2,453,005.400 (see Table 6), resulting in a rising rate of 0.1 mag hr^{-1}. The total magnitude change is about 0.8 mag in period 2, which is a factor of 2 larger than that in period 1, and the object appeared to be in an active or flaring state.

The most unusual variation in period 2 was observed on JD 2,453,006: all three light curves look very close to sine curves (see Fig. 3), with an amplitude of about 0.1 mag and a period of about 0.21 days (5 hr). This kind of variation is of particular interest and is discussed in § 3.4.

In order to establish whether there is a time lag between the variations in different wave bands, we have calculated the *z*-transformed discrete correlation function (Alexander 1997) for periods 1 and 2 and for several individual nights. No significant time lag has been identified, except that a couple of nights show time lags from a few to less than 20 minutes between different wave bands. A time lag between variations in different wave bands will lead to an oscillating color index with respect to brightness rather than the bluer-when-brighter trend reported in § 3.3.

In both periods the light curves in different bands are consistent with one another. The rms values of the differential magnitudes between the fifth comparison star and the average of all eight are 0.011, 0.010, 0.012, 0.009, 0.008, and 0.010 mag in the six small panels in Figures 2 and 3, respectively. These results demonstrate the accuracy of our magnitude measurements.

3.2. *Timescales of Variability*

A structure function (Simonetti et al. 1985) can be used to search for the typical timescales and periodicities of the variability. The characteristic timescale in a light curve, defined as the time interval between a maximum and an adjacent minimum or vice versa, is indicated by a maximum of the structure function, whereas the periodicity in a light curve causes a minimum of the structure function (Heidt & Wagner 1996).

For S5 0716+714, structure function analysis was performed on the light curves of each individual night. Short timescales of a few hours were derived, but the results were different from night to night. For example, the structure function analysis (see Fig. 4, *left*) identified a timescale of 0.11 days (2.5 hr) and a period of 0.21 days (5 hr) for JD 2,453,006, which is consistent with the period clearly visible for the sinelike light curves on that night. Another example is that the same analysis on the light curves of JD 2,453,007 revealed timescales of 0.07 and 0.17 days (1.7 and 4.1 hr) and periods of 0.11 and 0.23 days (2.6 and 5.5 hr; see Fig. 4, *right*). All timescales and periods are shown by dashed lines in Figure 4. There is also a common timescale of about 20 minutes in all structure functions, but this timescale is identical to the temporal resolution of our monitoring and cannot be associated with the intrinsic variability.

IDV has been frequently reported at radio and optical wavelengths in BL Lac object S5 0716+714; our observations at optical bands reconfirmed such IDV phenomena in this source. Instead of the much longer optical timescales of 4–10 days derived by other authors (e.g., Heidt & Wagner 1996; Qian et al. 2002), our dense monitoring enabled us to derive much shorter timescales for this object, which may constrain the physical processes that result in its fast microvariability (see discussion in § 3.4).

3.3. *Spectral Behavior*

The optical spectral change with brightness has been investigated for S5 0716+714 (e.g., Ghisellini et al. 1997; Raiteri et al. 2003; Villata et al. 2000, 2004) and for other BL Lac objects (e.g., Carini et al. 1992; Romero et al. 2000; Speziali & Natali 1998; Villata et al. 2002). Most authors have reported a bluer-when-brighter chromatism when the objects show fast flares and an "achromatic" trend for their long-term variability. However, Raiteri et al. (2003) also noted for S5 0716+714 that, on short timescales, "different behaviours have been found: sometimes a bluer-when-brighter trend is recognizable, while in some other cases the opposite is true; there are also cases where magnitude variations do not imply spectral changes." They suggested very dense monitoring with high-precision data to distinguish trends in the short-term spectral behavior of this source.

Our monitoring of S5 0716+714 with high temporal resolution enables us to study its spectral behavior with a high confidence level. Following most authors mentioned above, we

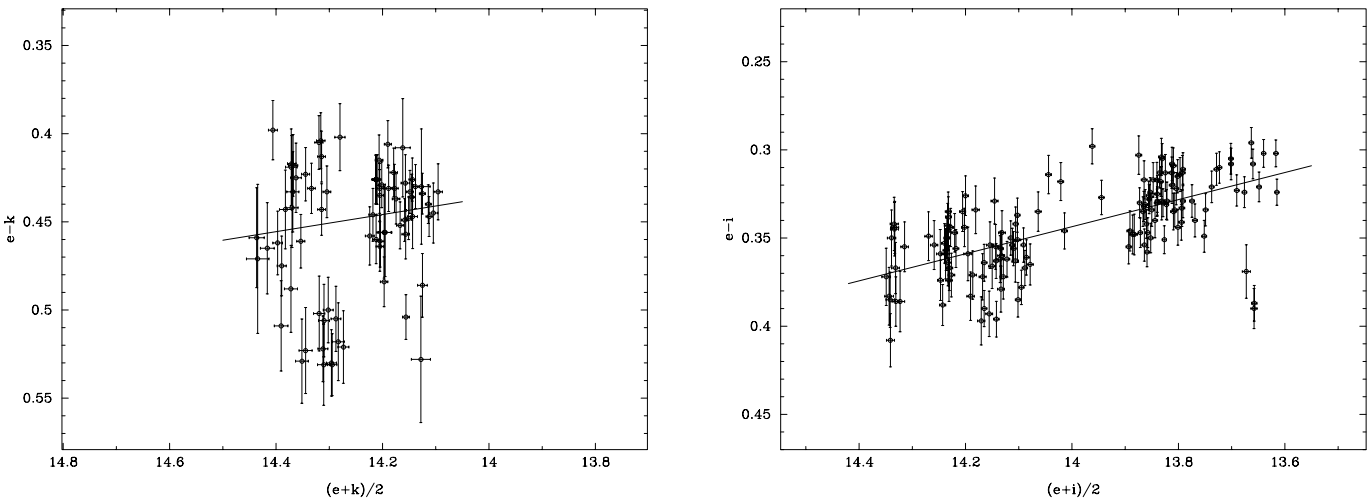

FIG. 5.—Color index vs. brightness in the two periods. The lines are best fits to the points. The bluer-when-brighter chromatism is clear in period 2 (*right*) but absent in period 1 (*left*). The two panels are set to have the same scales on both coordinates for comparison.

use the color index to denote the spectral shape. The color index and brightness are taken as $e - k$ and $(e + k)/2$ for period 1 and $e - i$ and $(e + i)/2$ for period 2. The changes of the color index with brightness in the two periods are shown in Figure 5. The solid lines show the best fits to the points and take the errors in both coordinates into consideration (Press et al. 1992).

In period 1, or when the object was in a relatively quiescent state, the distribution in the color-brightness diagram is quite dispersed, and there is not an overall color change. However, in period 2, or when the object was in a flaring state, a clear bluer-when-brighter chromatism is found. The linear fit has a slope of 0.077. The Pearson correlation coefficient is 0.636, and the significance level is 5.014×10^{-18}, suggesting a strong correlation between color index and brightness. This is in agreement with the results obtained by most authors mentioned above. Ghisellini et al. (1997) have deduced from their monitoring that two processes may be operating in this source: the first one would cause the achromatic long-term flux variations, while the second would be responsible for the short-term fast variations. Our results are somewhat different but still consistent with theirs; during the quiescent or low state, the variation may be dominated by the long-term component and does not show an overall spectral change, while in the active or flaring state, the variation is dominated by the short-term component and has a bluer-when-brighter chromatism.

That the spectra of S5 0716+714 change with its brightness has been observed at other wavelengths. For instance, Raiteri et al. (2003) reported a flatter-when-brighter trend in the radio wave band, and Cappi et al. (1994) discovered a steeper-when-fainter phenomenon in the soft X-ray. In fact, the spectrum changing with the flux at multiple wavelengths is a common feature in blazars (e.g., Aller et al. 1985; Urry et al. 1986; Sembay et al. 1993; Kniffen et al. 1993; Mukherjee et al. 1996). This universal spectral behavior is nontrivial. It suggests a close relationship between the mechanisms responsible for the emission and variation in different wave bands. The analysis of spectral changes of blazars can put some strong constraints on the physical processes that are responsible for these variations (see discussion in § 3.4).

3.4. *The Sine Light Curves*

The perfect sine light curves observed on JD 2,453,006 are of particular interest because very few of this kind of light curve have been reported before. They mimic a periodic variation, but there is only one complete period (it is a great pity that our weather became bad just at the end of this period). Webb (1990) detected a sinusoidal component in the variations of 3C 120, but the period was much longer (∼13 yr). For S5 0716+714, quasi-periodic oscillations have been detected by Quirrenbach et al. (1991). Their light curves, however, are very different: they are sawtooth-like with sharp turnoffs, while our light curves are sinelike with smooth turns. Therefore, we come to the question: What mechanism can produce such sinelike light curves?

Some mechanisms have been proposed to explain the IDV phenomena of blazars. They can be largely classified into two types, extrinsic and intrinsic, as reviewed by Wagner & Witzel (1995). The extrinsic mechanisms include interstellar scintillation (ISS) and gravitational microlensing. ISS is highly frequency dependent and only operates at low radio frequencies. The IDV in the millimeter regime and the fast variability in the optical regime, as observed by us, cannot be caused by the ISS mechanism. On the other hand, microlensing is an achromatic process and results in symmetric light curves. However, color or spectral changes have been frequently observed in radio to X-ray wave bands for S5 0716+714, as mentioned in § 3.3. We have also detected a clear bluer-when-brighter chromatism. In addition, the light curves at all wavelengths, including our optical ones, are generally asymmetric. Therefore, the fast variation of S5 0716+714 is not likely to be due to microlensing. In fact, the close correlation between the optical and radio bands observed in S5 0716+714 (e.g., Quirrenbach et al. 1991; Wagner et al. 1996) provides strong evidence against an extrinsic origin for its variability.

The intrinsic interpretations mainly include accretion disk instabilities and the shock-in-jet model. The accretion disk model is able to explain some of the phenomena seen in the optical to X-ray range but cannot explain the radio IDV (e.g., Wagner & Witzel 1995). The most frequently cited model is the shock-in-jet model, which has been widely used to explain the variability of blazars and quasars (e.g., Guetta et al. 2004; Jia et al. 1998; Qian et al. 1991; Romero et al. 2000; Wagner & Witzel 1995; and references therein). The main idea of the model is that shocks propagate down the relativistic jet, whose plasma is hydromagnetically turbulent. At sites where the shocks encounter particles or magnetic field overdensities, the optical synchrotron emission is enhanced. The amplitude and timescale

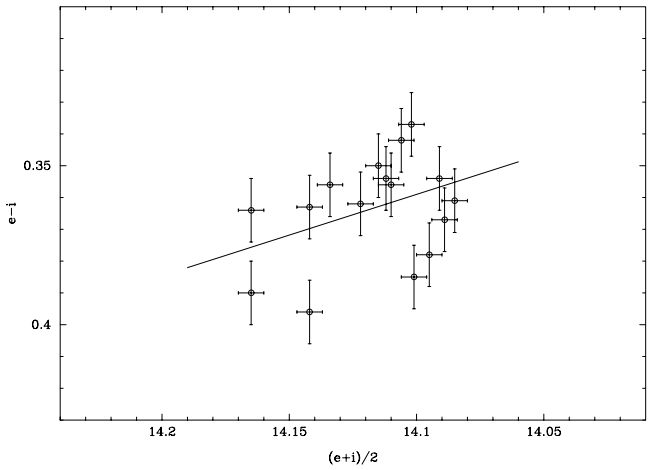

FIG. 6.—Color index vs. brightness on JD 2,453,006. The solid line indicates only a very weak correlation between the color index and brightness.

of the resulting variation depend on the power spectrum of the turbulence and the shock thickness. This kind of shock-in-jet model will naturally lead to the prediction of a bluer-when-brighter phenomenon (Marscher 1998), as observed in our case.

The shock-in-jet model still suffers from a number of problems in explaining IDV, such as the close correlation between the radio and optical variations. Therefore, geometric effects are sometimes invoked to account for some observational facts that cannot be interpreted satisfactorily by the shock-in-jet model. Geometric modulation in the context of shock-in-jet models is detailed by Camenzind & Krockenberger (1992). They argued that knots of enhanced particle density are injected at a finite jet radius. In knots moving relativistically on helical trajectories, the direction of forward beaming varies with time. For an observer close to the jet axis, the sweeping of the beam will introduce flares as a result of the lighthouse effect. This will lead to quasi-periodic variations of a few oscillations; the variations are basically achromatic.

It is tempting to examine the color change on only JD 2,453,006, since perfect sinelike light curves were observed on that night. Figure 6 illustrates the color index versus brightness relation. The linear fit gives a slope of 0.256, which is very different from the overall slope of period 2. The correlation coefficient is 0.361, and the significance level is 0.170, which means a poor fit or no clear correlation between the color index and brightness. That is to say, the brightness changed nearly achromatically on JD 2,453,006. The only two known processes that can cause achromatic variability are microlensing and the lighthouse effect. Although microlensing has been ruled out as the dominant mechanism of the variability of S5 0716+714, it may still make some contribution. The symmetry in the sine light curves may indicate a microlensing event, but the concave shape of the second halves of the light curves cannot be explained in terms of microlensing. In addition, this very short timescale would require a transverse speed of $v_{\rm trans} \sim c$ when microlensing. Therefore, the most probable mechanism responsible for the sine light curves is the lighthouse effect. It may produce a periodic variation according to Camenzind & Krockenberger (1992); the variation is achromatic. In other words, the variation observed on JD 2,453,006 is likely due to geometric effects.

It is unclear whether all fast IDVs, especially the quasi-periodic ones such as those observed by Quirrenbach et al. (1991), can also be explained in terms of geometric effects within the context of the shock-in-jet model. If the answer is yes, the actual timescales of the intrinsic flux changes will be longer by a factor of a few, and the deduced extremely high brightness temperature will be reduced by 1 or more orders of magnitude. This will help to resolve the large difference between the high brightness temperature ($\sim 10^{17}$ K) and the Compton limit ($< 10^{12}$ K), although not completely.

4. SUMMARY

During the periods of 2003 November 8–18 and 2003 December 30 to 2004 January 5, we carried out optical monitoring of the BL Lac object S5 0716+714 with a high temporal resolution. Intraday and intranight variations were observed, showing an overall magnitude change of about 0.9 mag during the whole campaign. Two outbursts were recorded on JD 2,453,005 and 2,453,009. Short timescales of a few hours were derived from the light curves of each individual night, but they were different from night to night. A bluer-when-brighter chromatism was present when the object was in an active or flaring state but was absent when it was in a relatively low or quiescent state.

Our observations have suggested that the fast microvariability in S5 0716+714 is basically consistent with the shock-in-jet model. The analysis has also indicated that geometric effects can sometimes play an important role in the variability of blazars. Up to now, all theoretical models that have been proposed to explain the variability of blazars have their own individual difficulties (see, e.g., Wagner & Witzel 1995 for a discussion). In order to better understand the variability of blazars and to strictly constrain the theoretical models, simultaneous multifrequency campaigns with high temporal resolution should be the direction of future efforts.

The authors thank the anonymous referee for valuable comments and suggestions that helped to improve this paper very much. This work has been supported by the Chinese National Key Basic Research Science Foundation (NKBRSF TG199075402) and in part by the National Natural Science Foundation of China (NSFC), grants 10303003 and 10473012. B. P. acknowledges grant NKBRSF 2003CB716703 and NSFC grant 10173015.

REFERENCES

Alexander, T. 1997, in Astronomical Time Series, ed. D. Maoz, A. Sternberg, & E. M. Leibowitz (Dordrecht: Kluwer), 163
Aller, H. D., Aller, M. F., Latimer, G. E., & Hodge, P. E. 1985, ApJS, 59, 513
Bertin, E., & Arnouts, S. 1996, A&AS, 117, 393
Buckley, J. H., et al. 1996, ApJ, 472, L9
Camenzind, M., & Krockenberger, M. 1992, A&A, 255, 59
Cappi, M., Comastri, A., Molendi, S., Palumbo, G. C. C., della Ceca, R., & Maccacaro, T. 1994, MNRAS, 271, 438
Carini, M. T., Miller, H. R., Noble, J. C., & Goodrich, B. D. 1992, AJ, 104, 15
Ghisellini, G., et al. 1997, A&A, 327, 61
Guetta, D., Ghisellini, G., Lazzati, D., & Celotti, A. 2004, A&A, 421, 877
Heidt, J., & Wagner, S. J. 1996, A&A, 305, 42
Jia, G. B., Cen, X. F., Ma, H. Y., & Wang, J. C. 1998, A&AS, 129, 569
Kniffen, D. A., et al. 1993, ApJ, 411, 133
Marscher, A. P. 1998, in Multifrequency Monitoring of Blazars, ed. G. Tosti & L. O. Takalo (Perugia: Publ. Oss. Astron. Univ. Perugia), 81
Mukherjee, R., et al. 1996, ApJ, 470, 831
Nesci, R., Massaro, E., & Montagni, F. 2002, Publ. Astron. Soc. Australia, 19, 143
Peng, B., Wu, J., & Zhou, X. 2003, MNRAS, 346, 483
Press, W. H., Teukolsky, S. A., Vetterling, W. T., & Flannery, B. P. 1992, in Numerical Recipes (2nd ed.; Cambridge: Cambridge Univ. Press), 660

Qian, B., Tao, J., & Fan, J. 2002, AJ, 123, 678
Qian, S. J., Quirrenbach, A., Witzel, A., Krichbaum, T. P., Hummel, C. A., & Zensus, J. A. 1991, A&A, 241, 15
Quirrenbach, A., et al. 1991, ApJ, 372, L71
Raiteri, C. M., et al. 2003, A&A, 402, 151
Romero, G. E., Cellone, S. A., & Combi, J. A. 2000, AJ, 120, 1192
Sembay, S., Warwick, R. S., Urry, C. M., Sokoloski, J., George, I. M., Makino, F., Ohashi, T., & Tashiro, M. 1993, ApJ, 404, 112
Simonetti, J. H., Cordes, J. M., & Heeschen, D. S. 1985, ApJ, 296, 46
Speziali, R., & Natali, G. 1998, A&A, 339, 382
Ulrich, M., Maraschi, L., & Urry, C. M. 1997, ARA&A, 35, 445
Urry, C. M., Mushotzky, R. F., & Holt, S. S. 1986, ApJ, 305, 369
Urry, C. M., et al. 1997, ApJ, 486, 799
Villata, M., Raiteri, C. M., Lanteri, L., Sobrito, G., & Cavallone, M. 1998, A&AS, 130, 305
Villata, M., et al. 2000, A&A, 363, 108
———. 2002, A&A, 390, 407
———. 2004, A&A, 421, 103
Wagner, S. J., & Witzel, A. 1995, ARA&A, 33, 163
Wagner, S. J., et al. 1996, AJ, 111, 2187
Webb, J. R. 1990, AJ, 99, 49
Wehrle, A. E., et al. 1998, ApJ, 497, 178